T-cell acute lymphoblastic leukemias express a unique truncated FAT1 isoform that cooperates with NOTCH1 in leukemia development

Charles E. de Bock,[1,2] Michelle Down,[3] Kinsha Baidya,[4] Bram Sweron,[1,2] Andrew W. Boyd,[3] Mark Fiers,[5] Gordon F. Burns,[6] Timothy J. Molloy,[7] Richard B. Lock,[8] Jean Soulier,[9] Tom Taghon,[10] Pieter Van Vlierberghe,[11] Jan Cools,[1,2] Jeff Holst[12] and Rick F. Thorne[13,14*]*

[1]KU Leuven, Center for Human Genetics, Belgium; [2]VIB, Center for Cancer Biology, Leuven, Belgium; [3]Leukaemia Foundation Laboratory, QIMR-Berghofer Medical Research Institute, Brisbane, Australia; [4]School of Medical Sciences and Prince of Wales Clinical School, University of New South Wales, Sydney, Australia; [5]VIB-KU Leuven Center for Brain & Disease Research, Belgium; [6]Cancer Research Unit, The University of Newcastle, Callaghan, NSW, Australia; [7]St Vincent's Clinical School, Faculty of Medicine, University of New South Wales, Sydney, Australia; [8]Children's Cancer Institute, Lowy Cancer Research Centre, University of New South Wales, Sydney, Australia; [9]U944 INSERM and Hematology laboratory, St-Louis Hospital, APHP, Hematology University Institute, University Paris-Diderot, France; [10]Department of Diagnostic Sciences, Faculty of Medicine and Health Sciences, Ghent University, Belgium; [11]Center for Medical Genetics, Ghent University Hospital, Belgium Cancer Research Institute Ghent (CRIG), Belgium; [12]Translational Cancer Metabolism Laboratory, Lowy Cancer Research Centre, University of New South Wales, Sydney, Australia; [13]Translational Research Institute, Henan Provincial People's Hospital, School of Medicine, Henan University, Zhengzhou, China and [14]School of Environmental and Life Sciences, University of Newcastle, NSW, Australia.

*Correspondence: *RICK F. THORNE.*
Rick.Thorne@newcastle.edu.au.
CHARLES E. DE BOCK.
cdebock@ccia.org.au
doi:10.3324/haematol.2018.198424

Supplementary Material

Materials and Methods

5'RACE, Northern Blotting and real-time quantitative PCR

Total RNA extraction, Northern blotting, FAT1 probe generation for cell lines was carried out as described[1]. 5'RACE was carried out using the SMART RACE cDNA amplification kit (Clontech) according to the manufacturer's instructions with PCR amplicons cloned into pGEM-T easy (Promega) prior to Sanger Sequencing. RNA was extracted from primary patient B- and T-ALL samples from using Maxwell 16 System Cell LEV total RNA purification kit (Promega). RNA was reverse transcribed using M-MLV reverse transcriptase and oligo-dT primers (Promega). The real time quantitative PCR was carried out using GoTaq qPCR master mix (Promega) on the ViiA-7 Real-Time PCR system (ThermoFisher Scientific). Analysis, quality controls and CNRQ (Calibrated Normalized Relative Quantity) determination was carried out using qBase+ and HPRT and RPS18 reference genes (Biogazelle). The levels of full length FAT1 and ΔFAT1 were discretely measured by exploiting sequence differences. Primer sequences are found within **Supplementary Table S3**.

Electroporation, siRNA and Western blotting

For electroporation, HPB-ALL cells were resuspended in 400 μL of serum free media containing 200 nmol siRNA (NOTCH1 Stealth siRNA HSS107249, FAT1 Stealth siRNA Exon2:HSS103567; exon 27 HSS103568; Custom intronic FAT1 siRNA sequence: 5'-UCCUUGGCAGGUGUCAGAGUGAUAU-3', ThermoFisher) and then transferred to 4 mm cuvettes (GenePulser Xcell, Bio Rad). T-ALL cell lines were electroporated (conditions listed in **Supplementary Table S4**) and allowed to recover for 24-48 hours in RPMI media with 20% FCS. For protein extraction, cells were lysed in either NDE lysis buffer (1% Nonidet P-40, 0.4% sodium deoxycholate, 66 mM EDTA, 10 mM Tris-HCl, pH 7.4) or 1X Cell Lysis Buffer (Cell Signaling Technology) supplemented with protease and phosphatase inhibitors (Complete protease inhibitor mixture and PhosSTOP, respectively; Roche Applied Science). Immunoprecipitation

and Western blotting was carried as previously described [1] with the following modifications. Immunoprecipitates were collected using magnetic protein-G beads (Cell Signaling Technology). Lysates were applied to commercial 3–8% Tris acetate and run in 1X MES buffer (Invitrogen) and proteins transferred to PVDF membranes (iBlot Transfer Stack and iBlot device, Invitrogen).

CRISPR/Cas9 targeting of FAT1

The pX330 vector containing the gRNA to exon 1 of FAT1 was obtained from Dominique Kranz[2]. For electroporation, 1 x 10^6 Jurkat cells resuspended in serum free media and electroporated with 10 ug of DNA using 8 pulses at 175V (Pulse length = 2.5 ms, pulse interval 0.1 s) in 2mm cuvettes and the square wave function (GenePulser Xcell, Bio Rad). Cells were then plated at low density in ClonaCell-TCS media (STEMCELL Technologies). After 2 weeks, single colonies were picked manually and expanded. Loss of FAT1 was assessed for each clone by Western blot analysis.

In vitro assays

Cell proliferation was assessed in 96 well plates over 4 days by sequential scans of GFP fluorescent signals using a Fuji Typhoon instrument (488 laser with filter 520BP40; 300 PMT and high sensitivity). Densitometric values for each well were derived using Multigauge (changing the range scope to 1-1000) and values normalized against day 1. Foci and soft agar assays were performed in 6 well plates as described previously [3,4] . Colonies were visualised by staining with 0.005% (w/v) crystal violet.

Murine Bone Marrow transplantation

Retrovirus production and murine bone marrow transplantation using CD2-Cre mice was carried out as previously described[5]. Briefly, male CD2-Cre donor mice were sacrificed and bone marrow cells were harvested from femur and tibia. Lineage negative cells were enriched (STEMCELL Technologies) and cultured overnight in RPMI with 20% FCS with IL3 (10 ng/mL, Peprotech), IL6 (10 ng/mL, Peprotech), SCF (50 ng/mL, Peprotech), and penicillin-streptomycin. The following day, 1x10^6 cells

were transduced by spinoculation (90 min at 2500rpm) with viral supernatant and 8 μg/mL polybrene. The following day, the cells were washed in PBS and injected (1×10^6 cells/0.3 mL) into the lateral tail vein of sub-lethally irradiated (5 Gy) syngeneic female C57BL/6 recipient mice. Mice were housed in IVC cages and monitored daily. Bone marrow transplant using C57BL/6 donor cells and Rag1-/- recipients was carried out as described[6].

In silico microarray, ChIP seq and subcellular localization analysis

Gene expression analysis of T-cell subsets and primary T-ALL samples was performed as previously described[7]. Microarray data have been deposited in the GEO (https://www.ncbi.nlm.nih.gov/geo/) with accession number GSE62156. ChIP-seq data were downloaded from GEO and analysed using IGV. Jurkat data were downloaded from datasets GSE23080, GSE60104, GSM1697882, GSM2064702. HeLa data was downloaded from GSE29611. Histone marks for T-ALL cell lines were downloaded from GSE76783, GSM1442003 and GSM1246865. 293T data was downloaded from GSE51633. MDA-MB-231 data was downloaded from GSE72141 and GSM1824910. Subcellular localization analysis was carried out using DeepLoc-1.0 (http://www.cbs.dtu.dk/services/DeepLoc-1.0/).

Ethical aspects

Animal experiments were approved by the Ethical committee on animal experimentation of KU Leuven. Human leukemia samples were collected at the University Hospital Leuven (UZ Leuven) after approval by the ethical committee. Informed consent was obtained from all patients or their parents, according to the Declaration of Helsinki.

References

1. Sadeqzadeh E, de Bock CE, Zhang XD, Shipman KL, Scott NM, Song C, et al. Dual processing of FAT1 cadherin protein by human melanoma cells generates distinct protein products. J Biol Chem. 2011 Aug 12;286(32):28181–91.

2. Kranz D, Boutros M. A synthetic lethal screen identifies FAT1 as an antagonist of caspase-8 in extrinsic apoptosis. EMBO J. 2014 Feb 3;33(3):181–97.

3. Guo ST, Jiang CC, Wang GP, Li YP, Wang CY, Guo XY, et al. MicroRNA-497 targets insulin-like growth factor 1 receptor and has a tumour suppressive role in human colorectal cancer. Oncogene. Nature Publishing Group; 2012 Jun 18;32(15):1910–20.

4. Oliveira CS, de Bock CE, Molloy TJ, Sadeqzadeh E, Geng XY, Hersey P, et al. Macrophage migration inhibitory factor engages PI3K/Akt signalling and is a prognostic factor in metastatic melanoma. BMC Cancer. BioMed Central; 2014 Dec 1;14(1):630.

5. de Bock CE, Demeyer S, Degryse S, Verbeke D, Sweron B, Gielen O, et al. HOXA9 cooperates with activated JAK/STAT signaling to drive leukemia development. Cancer Discov. American Association for Cancer Research; 2018 Mar 1;:CD–17–0583.

6. Holst J, Vignali KM, Burton AR, Vignali DAA. Rapid analysis of T-cell selection in vivo using T cell-receptor retrogenic mice. Nat Methods. Nature Publishing Group; 2006 Mar;3(3):191–7.

7. Peirs S, Matthijssens F, Goossens S, Van de Walle I, Ruggero K, de Bock CE, et al. ABT-199 mediated inhibition of BCL-2 as a novel therapeutic strategy in T-cell acute lymphoblastic leukemia. Blood. 2014;124(25):3738–47.

Supplementary Tables

Supplementary Table S1: 5'RACE sequences cloned and sequenced from pGEM-T vectors

Clone Number	Sequence in pGEM-T
J2.1	1 GGACAAAGTG GAGTCGACAT TCTTCGTACT GCTTTGAACA GATGTGATGA TCTCCTTTCT 61 TAAATCTTTA CATGTTTGAG AGGCTGAGGC AGNAGGATCA CTTGAGGCTA GAAGTGAGGC 121 AGCCTGGGCG TTACAGGGAA ACCCCATCTC TACAAAAACT TAAAAAATCA GCCAGGCATG 181 TGGCATGCCT CTAGTTCCAG CTACTCAGGA GGCTGAGGTG GGAGGATCCC TGAGCCCGGG 241 AGTTTGAGGA TGCAATGAGC TGAGATTGCG CCACTGCACT CCAGCCTGGG TGGCAGAGCG 301 AGACCCTGTC TCAAAAAATA AAAATATTGA AAGGTTATTA CTGCAAATGC AGTGCCTTGT 361 ACATAGGGAC CCACTGTGAG ATAAGCGTCA ATCCGTGTTC CTCCAACCCA TGCCTCTATG 421 GGGGCACGTG TGTTGCCGAC AACGGAGGCT TTGTTTGCCA GTGTAGAGGA TTATATACTG 481 GTCAGAGG TG TCAGCTTAGT CCATACTGCA AAGATGAACC CTGTAAGAAT GGCGGAACAT 541 GCTTTGACAG TTTGGATGGC GCCGTTTGTC AGTGTGATTC GGGTTTTAGG GGAGAAAGGT 601 GTCAGAGTGA TATCGACGAG TGCTCTGGAA ACCCTTGCCT GCACGGGGCC CTCTGTGAGA 661 ACACGCACGN CTCCTANCAC TGCAACTGC
J3.1[#]	1 GCAGTCTNTA AGGATTGAGC CTGACATACG CTGGCGT**ATG** CTACAGAGGT CTCTCCTCAT 61 TCCTGACTTC CTTGGCAGGT GTCAGAGTGA TATCGACGAG TGCTCTGGAA ACCCTTGCCT 121 GCACGGGGCC CTCTGTGAGA ACACGCACGG CTCCTATCAC TGCAACTGCA

[#] Underlined sequence maps to intronic sequence directly upstream of exon 25 coding region. The putative start site within the retained intron is highlighted in bold text and exon 25 shaded yellow.

Supplementary Table S2: Primary B- and T-ALL patient characteristics

Patient	Disease	Molecular diagnostics
X00	pre-B-ALL	N/A
X01	pre-B-ALL	N/A
X09	mature T-ALL	*NOTCH1, NRAS, SPI1-TCF7*, del(9p), t(14q11)
X10	T-ALL	*NOTCH1*, *BCL11B*, *DNM2*, del(9p), possible heterozygous loss *RB1*
X11	T-ALL	*PTPRC, SETD2, WT1, CTCF, JAK3* (M551I), *EP300, PHF6*, loss *CDKN2B*
X12	T-ALL	*PTPRC, ETV5, FBXW7*, loss *CDKN2B*
X13	T-ALL	NOTCH1(F1592S), DCLER1C (F522S); RPL10(R98S)
X14	T-ALL	WT1, NOTCH1, RPL10 (R98S), loss p16
X15	T-ALL	NOTCH1(L1593P); NOTCH1(D1533G); RPL10 (R98S); del CDKN2B
X16	T-ALL	PTEN Fs, del p16
X17	T-ALL	PTEN Q214*
XA18	common B-ALL	del(9p) t(X;14)(p22;q34)
XA19	pre-B-ALL	del(9p) t(9;22)(q34;q11) der(9)t(8;9) *BCR-ABL1* e1a2
XA31	pre-B-ALL	*N/A*
XA32	T-ALL	del p16, heterozyg del PTPN2, NOTCH1 V2536I, TET2 I1762V, del ETV6, del WT1, del BCL11B, SPI1 insertie C204*, CNOT1 insertie F1543*
XB34	T-ALL	N/A

XB37	immature T-ALL	*STAT5B*, 2x *NOTCH1, BCL11B, CDKN2A, STIL-TAL1,* t(11;14)(p13;q11)
XB40	pre-B-ALL	*BCR-ABL1* e1a2
XB41	T-ALL	*NOTCH1, RPL10* (R98S), del(*TCRG*)
XB47	T-ALL	*NOTCH1* 2x, *RPL10* (R98S), *CNOT3* indel, del(9p), del(*TCRG*)
XC51	pre B-ALL	*BCR-ABL1* e1a2, del(*IKZF1* exon 4-7), del(*RB1* exon 19-26)
XC56	pre-B-ALL	*TCF3-PBX1* t(1;19)(q23;p13.3) del(9p)
XC57	T-ALL	*TAL1-TCRa/d*, del(9p)t(1;14)(p32;q11)
1Q94	T-ALL	DNM2(ins G→AG, 653V>MV); IL7R (fs); IL7R(242L>LF); NOTCH1 (insG fs)
382L	T-ALL	JAK3(R657Q); SETD2 (E1043G); CNOT3(fs); JAK1(R724H); EED (splice); PHF6(G291R); TCOF1(P1379Q); ODZ2(K558E); LSG1(M520V).
389E	T-ALL	DNM2 (splice); JAK3(M511I); NOTCH1(L1600P)
7Q05	T-ALL	DNM2(delAGA); JAK3(M511I); CDKN2A(del); AKAP6(A1313G); PHF6 (del), NOTCH1(Y1619H, M1615T); FBXW7(R689W)
839U	T-ALL	IL7R(insGG); TET1(648R>RG); RPL5 (insCC fs); RPL5(G>AG, 35R>HR)
863I	T-ALL	CDKN1B(73K>NK); CNOT2(448Y>HY); LEF1(fs;325E>EQ); NOTCH1(fs)
9H60	T-ALL	NOTCH1(L1593P); IL7R(418P>PA); BCL11B (fs); RPL10(R98S)
O623	T-ALL	JAK3(L857P); WT1(S280N); STAT5A(P194L); ZFP36L2 (inframe insertion ins CTGCTC); SETD2(S175A)

Supplementary Table S3: qPCR primers

Gene	Direction	Primer sequence
FAT1 (Exon 2/3)	Forward	GACGCAGACATCCGCTCTAA
	Reverse	AAACAGCTTGCTCCTCACGA
ΔFAT1	Forward	CCTCATTCCTGACTTCCTTGG
	Reverse	CTGTACTCGTGGCTGCAGTT
MYC	Forward	AAAACCAGCAGCCTCCCGCGA
	Reverse	AATACGGCTGCACCGAGTCGT
NOTCH1	Forward	CCGTAGATGACCTGGGCAAG
	Reverse	CCAGAAACAGGGGTGTCTCC
HPRT	Forward	TGACACTGGCAAAACAATGCA
	Reverse	GGTCCTTTTCACCAGCAAGCT
RPS18	Forward	TAG CCT TTG CCA TCA CTG CC
	Reverse	CAT GAG CAT ATC TTC GGC CC

Supplementary Table S4: Electroporation conditions for T-ALL cell lines and siRNA

Cell line	Conditions
HPB-ALL	Exponential decay, 300V, 500 μF
ALL-SIL	Exponential decay, 275V, 1000 μF
CCRF-CEM	Exponential decay, 300V, 950 μF
KE37	Exponential decay, 300V, 950 μF

Supplementary Figure S1: In silico analysis of FAT1 levels in ETP vs non-ETP-T-ALL samples
The publically-available microarray gene expression dataset GSE28703 was analysed using GEO2R for FAT1 expression. Plots show mean and standard deviation (Mann Whitney t-test, $p < 0.001$).

Supplementary Figure S2: Northern blot analysis with different FAT1 exon probes. A, Northern blot using alternative exon probes in LK63 (preB-ALL cell line) and Jurkat (T-ALL cell line). **B,** Summary schematic of Northern blotting results in Jurkat cell line in comparison with the original probe used by Dunne et al. **C,** Northern blot comparing HuT78 and Jurkat to determine the exons expressed at the N-terminus of the mRNA transcript and corresponding **D,** RT-PCR of the FAT1 mRNA. **E,** Genomic DNA PCR across the loci to show there is no deletion in HuT78.

Supplementary Figure S3: ΔFAT1 protein is predicted to be localized to the cell membrane. Analysis of the predicted peptide sequence using DeepLoc-1.0 predicts that the protein will be at the cell membrane.

Supplementary Figure S4: H3K27Ac and H3K4me3 analysis of FAT1 locus. A, H3K27Ac ChIP-seq analysis of T-ALL cell lines. **B,** H3K4me3 and H3K27Ac ChIP-seq analysis at the FAT1 genomic loci for MDA-MB-231 and 293T cells.

Supplementary Figure S5: NIH-3T3 cell transformation assay after viral transduction with ΔFAT1. A, Western blot of NIH-3T3 for ΔFAT1 transgene expression. **B,** Cell proliferation of NIH-3T3 cells transduced with either pMIGII_empty GFP vector or pMIGII_ΔFAT1_IRES_GFP and then quantified using fluorescent scanning of GFP of adherent cells. **C.** Foci and Soft agar assay of pMIGII_empty GFP vector or pMIGII_ΔFAT1_IRES_GFP cells as indicated.

Supplementary Figure S6: Bone marrow transplant model of ΔFAT1 in Rag1$^{-/-}$ recipient mice. A, Schematic illustration of bone marrow transplant model**. B,** Flow cytometry analysis of peripheral blood of T-cells at day 200 post transplantation of both GFP^{+} and GFP^{-} populations. **C,** Flow cytometry analysis of peripheral blood of B-cell and myeloid cells at day 200 post transplantation of both GFP^{+} and GFP^{-} populations.

Supplementary Figure S7: NOTCH signalling in T-ALL cell lines after NOTCH1, FAT1 or ΔFAT1 siRNA mediated knockdown. Real time qPCR analysis after 24 h siRNA mediated knockdown in ALL-SIL, KE37 and CCRF-CEM T-ALL cell lines. Expression values were normalised to HPRT and 18S rRNA reference genes and then to negative control siRNA. Data plotted is mean normalised expression +/- SEM and is

collation of three independent experiments. Statistical analysis was calculated using t-test with equal variance assumption.

Supplementary Figure S8: Inducible ICN and ΔFAT1 analysis. A, Western blot of analysis of Ba/F-Cre cells transduced with virus constructs encoding either ICN only or ICN and ΔFAT1. Two different clones were analysis for ICN-P2A-ΔFAT1. **B,** Flow cytometry analysis of peripheral blood analysis at day 14 post injection and stained for CD4/CD8 indicative of Notch driven leukemia. Each plot represents a different mouse within the experiment.

Supplementary Figure S1

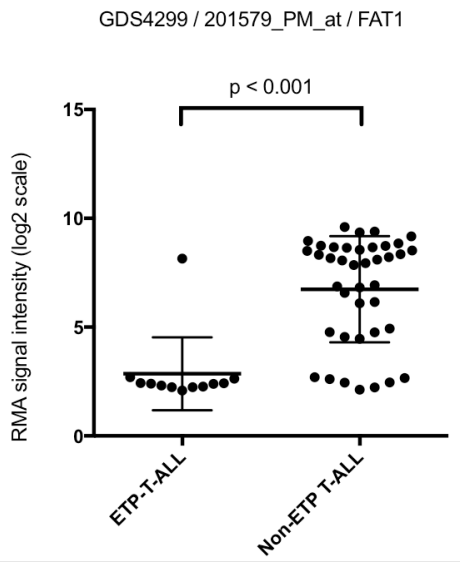

Supplementary Figure S2

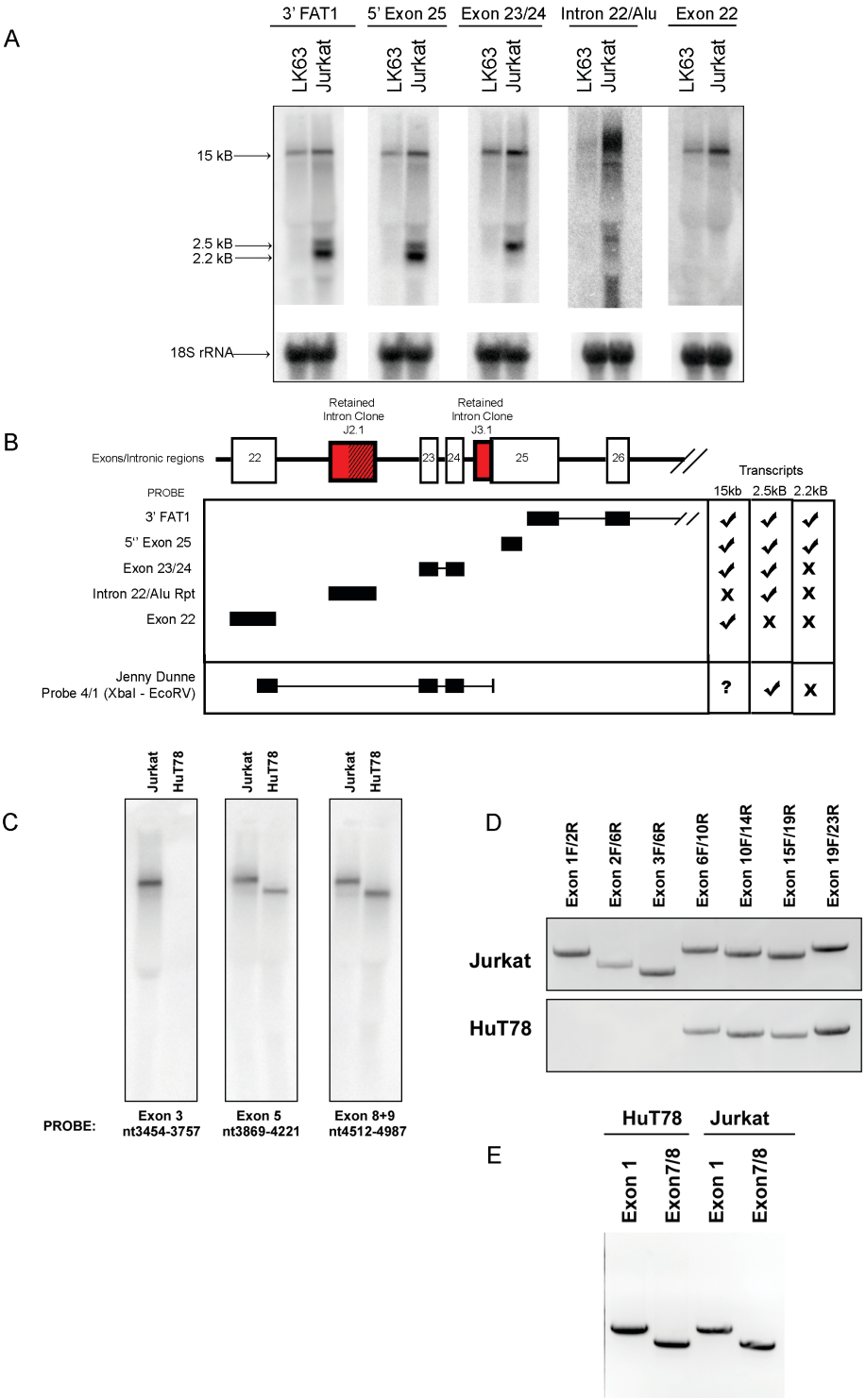

Supplementary Figure S3

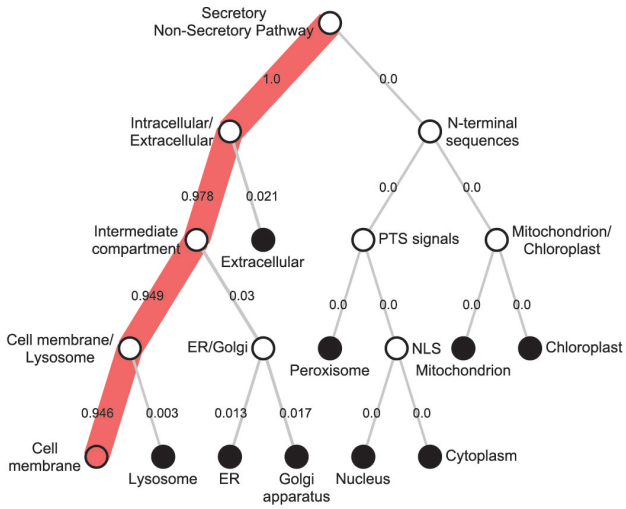

Localisation	Nucleus	Cytoplasm	Extracellular	Mitochondria	Cell Membrane	Endoplasmic Ret.	Golgi	Lysosome	Peroxisome
Likelihood	0	0	0.0087	0	0.9675	0.0077	0.0137	0.0024	0

Supplementary Figure S4

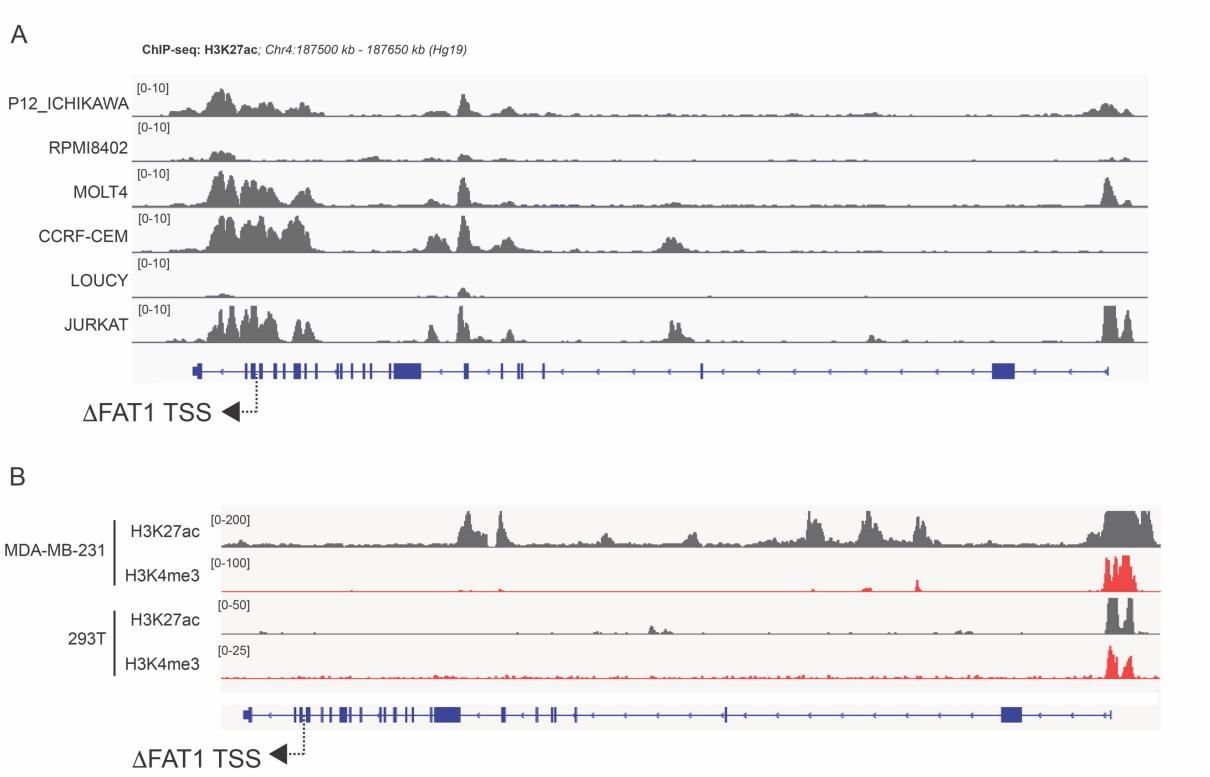

Supplementary Figure S5

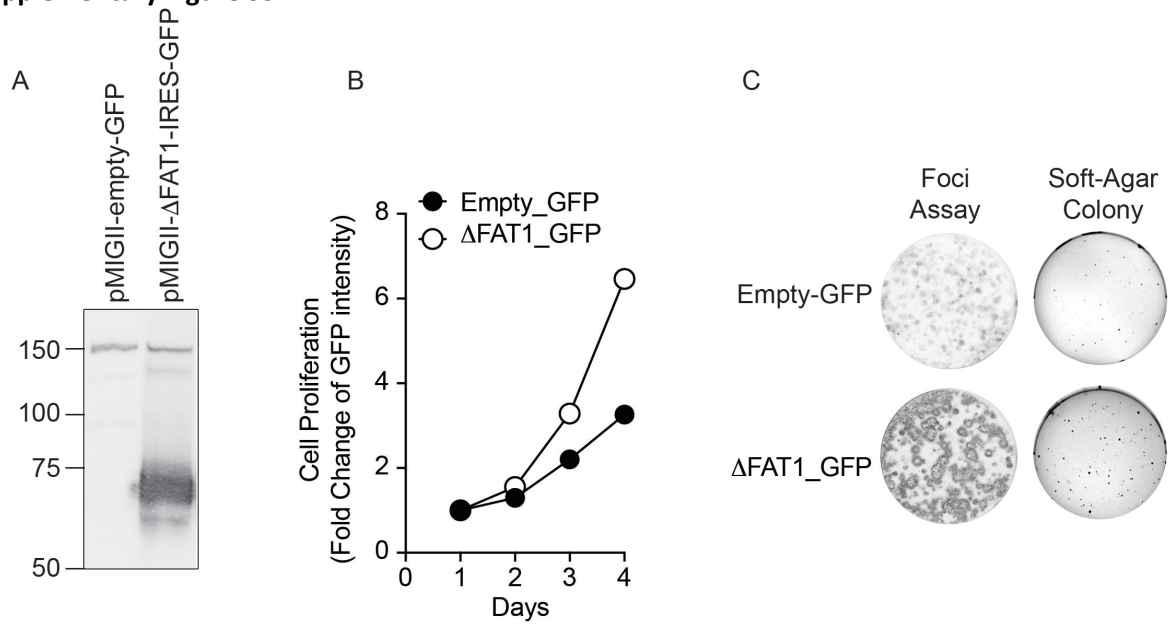

Supplementary Figure S6

A

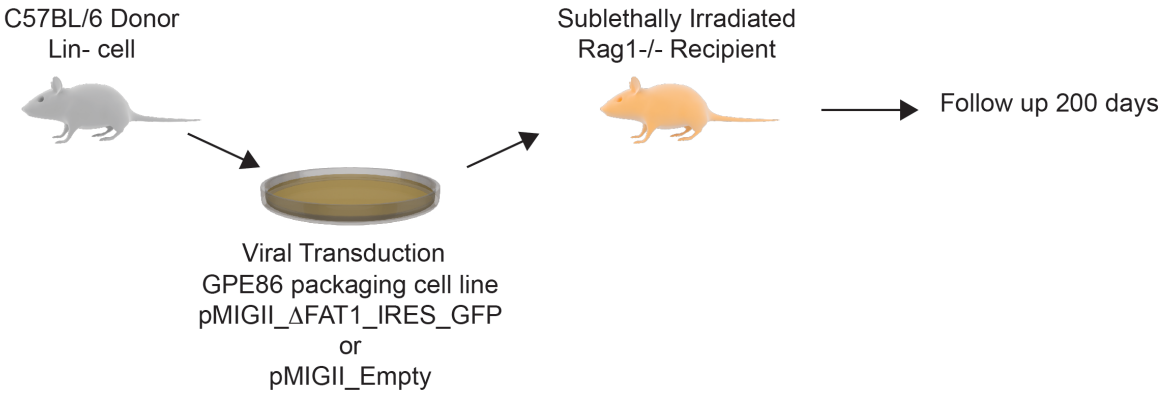

B

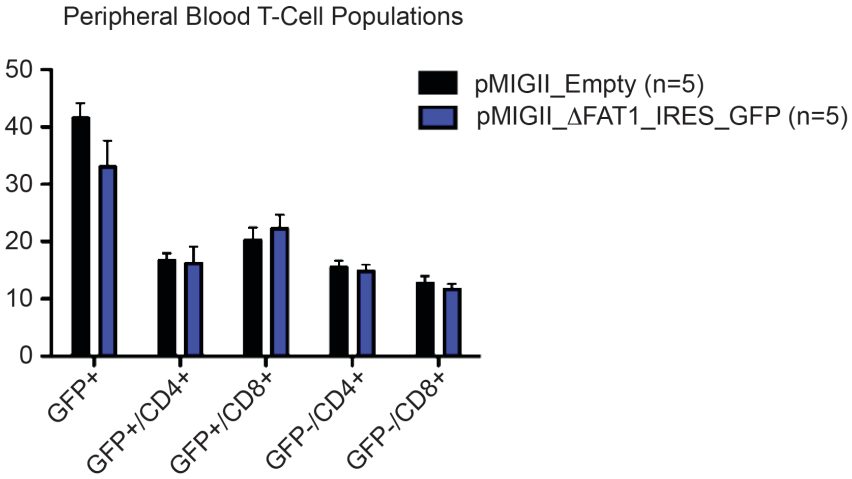

C

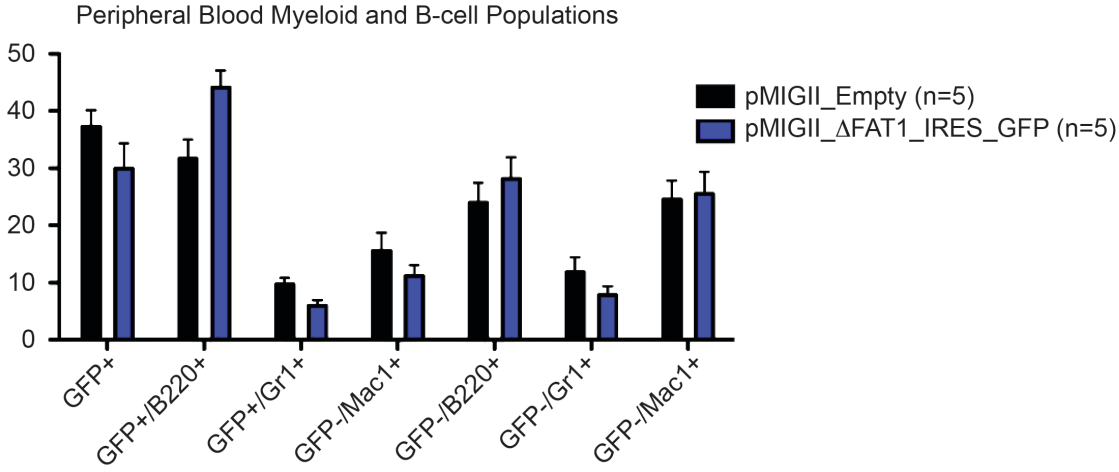

Supplementary Figure S7

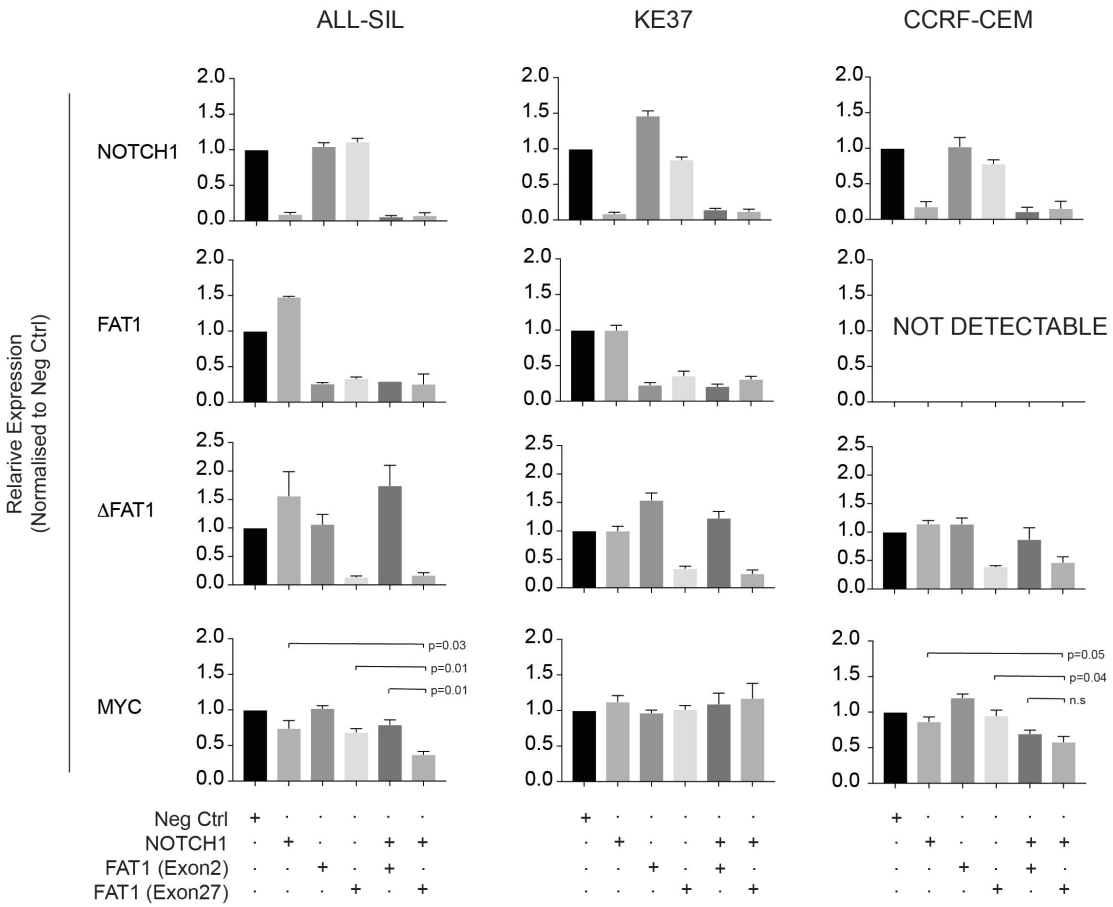

Supplementary Figure S8